ESC European Society of Cardiology

European Heart Journal - Cardiovascular Imaging (2021) **22**, 298–306
doi:10.1093/ehjci/jeaa224

Pericoronary adipose tissue computed tomography attenuation distinguishes different stages of coronary artery disease: a cross-sectional study

Andrew Lin [1,2,3], Nitesh Nerlekar[1,2], Jeremy Yuvaraj[1,2], Katrina Fernandes[1], Cathy Jiang[1], Stephen J. Nicholls[1,2], Damini Dey[3], and Dennis T.L. Wong[1,2]*

[1]Monash Cardiovascular Research Centre, Monash University and MonashHeart, Monash Health, 246 Clayton Road, Clayton, Victoria 3168, Australia; [2]Department of Medicine, Monash University, Clayton, Victoria, Australia; and [3]Biomedical Imaging Research Institute, Cedars-Sinai Medical Center, Los Angeles, CA, USA

Received 24 February 2020; editorial decision 16 July 2020; accepted 17 July 2020; online publish-ahead-of-print 27 August 2020

Aims Vascular inflammation inhibits local adipogenesis in pericoronary adipose tissue (PCAT) and this can be detected on coronary computed tomography angiography (CCTA) as an increase in CT attenuation of PCAT surrounding the proximal right coronary artery (RCA). In this cross-sectional study, we assessed the utility of PCAT CT attenuation as an imaging biomarker of coronary inflammation in distinguishing different stages of coronary artery disease (CAD).

Methods and results Sixty patients with acute myocardial infarction (MI) were prospectively recruited to undergo CCTA within 48 h of admission, prior to invasive angiography. These participants were matched to patients with stable CAD ($n = 60$) and controls with no CAD ($n = 60$) by age, gender, BMI, risk factors, medications, and CT tube voltage. PCAT attenuation around the proximal RCA was quantified per-patient using semi-automated software. Patients with MI had a higher PCAT attenuation (-82.3 ± 5.5 HU) compared with patients with stable CAD (-90.6 ± 5.7 HU, $P < 0.001$) and controls (-95.8 ± 6.2 HU, $P < 0.001$). PCAT attenuation was significantly increased in stable CAD patients over controls ($P = 0.01$). The association of PCAT attenuation with stage of CAD was independent of age, gender, cardiovascular risk factors, epicardial adipose tissue volume, and CCTA-derived quantitative plaque burden. No interaction was observed for clinical presentation (MI vs. stable CAD) and plaque burden on PCAT attenuation.

Conclusion PCAT CT attenuation as a quantitative measure of global coronary inflammation independently distinguishes patients with MI vs. stable CAD vs. no CAD. Future studies should assess whether this imaging biomarker can track patient responses to therapies in different stages of CAD.

Keywords coronary computed tomography angiography • pericoronary adipose tissue • inflammation • atherosclerosis • myocardial infarction

Introduction

Inflammation is a major driver of atherogenesis and atherothrombosis resulting in acute coronary syndrome (ACS).[1] Local inflammation within culprit coronary lesions has been demonstrated on intravascular imaging[2] and positron emission tomography–computed tomography (PET-CT)[3,4]. Furthermore, the landmark CANTOS (Canakinumab Anti-Inflammatory Thrombosis Outcomes Study) trial validated the inflammatory hypothesis of atherosclerosis in patients with stable coronary artery disease (CAD) and residual inflammatory

*Corresponding author. Tel: +61 (3) 9695 6666; Fax: +61 (3) 9594 4246. E-mail: dennis.wong@monash.edu
Published on behalf of the European Society of Cardiology. All rights reserved. © The Author(s) 2020. For permissions, please email: journals.permissions@oup.com.

risk.[5] It is established that vascular inflammation inhibits local adipogenesis in pericoronary adipose tissue (PCAT), enabling non-invasive detection on coronary computed tomography angiography (CCTA) as an increased CT attenuation [Hounsfield units (HU)] of PCAT surrounding the proximal right coronary artery (RCA).[6] Temporal changes in this metric associate with plaque progression or regression in stable CAD.[7] Further, a high PCAT attenuation confers an increased risk of cardiac mortality in patients with suspected CAD.[8] No studies to date have quantified PCAT attenuation around the proximal RCA in patients with myocardial infarction (MI). Moreover, the relationship between PCAT attenuation and different stages of CAD has not been systematically evaluated. In this cross-sectional study, we assess the value of PCAT attenuation as a non-invasive imaging biomarker of coronary inflammation in distinguishing patients with MI from patients with stable CAD and controls with no CAD.

Methods

Study population

Sixty consecutive patients admitted with acute MI from June 2018 to January 2019 at MonashHeart (Monash Medical Centre, Melbourne, Australia) were prospectively recruited to undergo CCTA within 48 h of admission, prior to invasive coronary angiography. We included patients with thrombolysed ST-segment elevation MI (STEMI) or non-ST-segment elevation MI (NSTEMI)[9] who had a culprit lesion identified by an interventional cardiologist at invasive angiography. Exclusion criteria included previous MI or revascularization, clinical or haemodynamic instability, severe renal impairment (eGFR <30 mL/m/1.73 m^2), or allergy to iodinated contrast. Participants with MI were matched to outpatients who underwent CCTA for suspected CAD during the same time period, stratified by two groups: (i) 60 patients with stable CAD (defined by the presence of stable exertional symptoms and/or inducible myocardial ischaemia on stress testing) and detection of stenosis severity 25–99% on CCTA; and (ii) 60 patients with no visually detectable CAD on CCTA who formed the control group. Matching of the three groups was performed for age, gender, body mass index (BMI), cardiovascular risk factors (diabetes, hypertension, dyslipidaemia, and smoking), medications, and CT tube voltage. The study had institutional ethics approval and all patients with MI provided written informed consent. The study was registered on the Australian New Zealand Clinical Trials Registry (http://www.anzctr.org.au. Unique identifier: ACTRN12618001058268). *Figure 1* details the patient selection and study design.

Definition of risk factors

Cardiovascular risk factors and medications were documented on admission for the MI cohort and obtained by review of electronic medical records and a pathology database for the outpatient cohorts. Diabetes mellitus was defined by a haemoglobin A1c ≥6.5% or use of diabetic medications. Hypertension was defined as a systolic blood pressure >140 mmHg or diastolic blood pressure >90 mmHg at the time of CCTA (outpatients only), or diagnosis/treatment of hypertension. Dyslipidaemia was defined as a fasting total cholesterol >6.2 mmol/L, low-density lipoprotein cholesterol (LDL-C) >3.4 mmol/L, high-density lipoprotein cholesterol <1.0 mmol/L, serum triglycerides >1.7 mmol/L[10] (outpatients only), or diagnosis/treatment of dyslipidaemia. Family history of CAD was defined as ≥1 first-degree relative with CAD before age 60 years. Smokers were eitheractive and former smokers.

CCTA acquisition

All scans were performed on a 320-detector-row CT scanner (Aquilion ONE ViSION, Canon Medical Systems, Japan) as previously described.[11] Prior to contrast injection, a non-contrast cardiac CT was performed. Sublingual nitroglycerine (0.4–0.8 mg) was administered immediately prior to CTA scanning. Iodinated contrast [60–90 mL, 350 mg iodine per mL (Omnipaque)] was injected at a flow rate of 5 mL/s. CTA was performed with prospective electrocardiogram-gating and automatic tube current modulation. Acquisition parameters were as follows: detector collimation 320 mm × 0.5 mm; 275 ms gantry rotation time; tube current 300–500 mA (depending on BMI); tube voltage 120 kV if BMI ≥25 kg/m^2 and 100 kV if BMI <25 kg/m^2. Images were reconstructed with a 512 × 512 matrix, 0.5 mm slice thickness, and 0.25 mm increments, using convolution kernel FC43 and iterative reconstruction (Adaptive Iterative Dose Reduction 3D, Canon Medical Systems, Otawara, Japan).

CCTA interpretation

CCTA images were analysed in axial and multi-planar reconstruction views. We excluded scans deemed uninterpretable due to artefact or heavy calcification [4 patients (5%) in MI cohort; 44 patients (2%) in outpatient cohort]. An expert CCTA reader (A.L.) blinded to clinical data performed visual assessment of all coronary segments ≥2 mm according to an 18-segment model.[12] Each segment was scored for the presence or absence of plaque (0: absent and 1: present) and degree of stenosis [0: none, 1: minimal (<25%), 2: mild (25–49%), 3: moderate (50–69%), 4: severe (70–99%), or 5: occlusion (100%)].[12] In each patient, segment involvement score (SIS) was the total number of segments with any plaque, and segment stenosis score (SSS) was the sum of the stenosis scores of each segment.[13] These indexes were used as qualitative measures of CAD extent and severity.

Coronary plaque quantification

For the MI and stable CAD cohorts, quantitative plaque assessment was performed at the Cedars-Sinai Medical Center core laboratory by the same blinded reader using semi-automated software (Autoplaque v2.5, Cedars-Sinai Medical Center, Los Angeles, CA, USA). In multi-planar views, the luminal centreline was manually defined with 5–7 control points and a region of interest was placed in the ascending aorta to define normal blood pool. After marking the proximal and distal lesion limits of the lesions, plaque quantification was fully automated according to adaptive scan-specific thresholds.[14] Plaque volume was calculated on a per-lesion level by summing the volumes of non-calcified and calcified plaque components. Measurements across the entire coronary tree were totalled on a per-patient level. Coronary plaque burden was calculated as: plaque volume × 100%/analysed vessel volume. Depending on the image quality and number of coronary lesions, the per-patient processing time for complete plaque analysis of the coronary tree ranged between 10 and 60 min. The per-lesion processing time ranged between 3 and 7 min, depending on plaque features such as location, length and burden. *Figure 2* demonstrates a case example of semi-automated plaque quantification.

PCAT quantification

Measurement of PCAT attenuation around the proximal RCA is a standardized method which has been used in prior studies as a representative biomarker of coronary inflammation.[6–8,15] Hence, we focused on the proximal RCA (10–50 mm from RCA ostium) for our per-patient level PCAT attenuation analysis. After performing plaque quantification in this segment, CT analysis of PCAT was fully automated (Autoplaque v2.5). PCAT was sampled in 3D layers, moving radially outwards from the coronary wall in 1 mm increments. Adipose

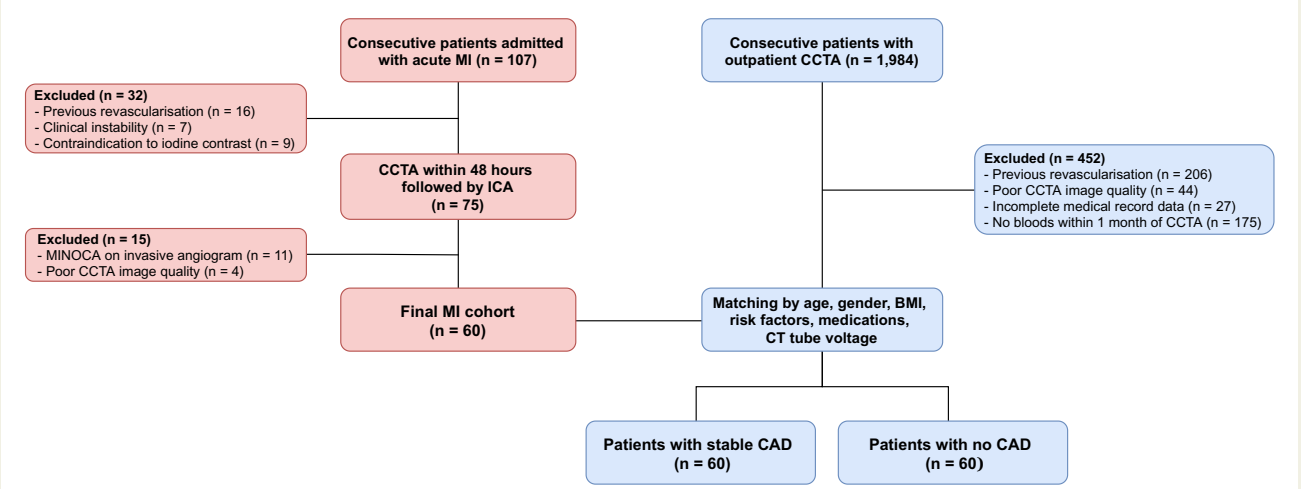

Figure 1 Patient selection and study design. Flow chart showing inclusion and exclusion criteria for the three cohorts. BMI, body mass index; ICA, invasive coronary angiography; MINOCA, myocardial infarction with non-obstructive coronaries.

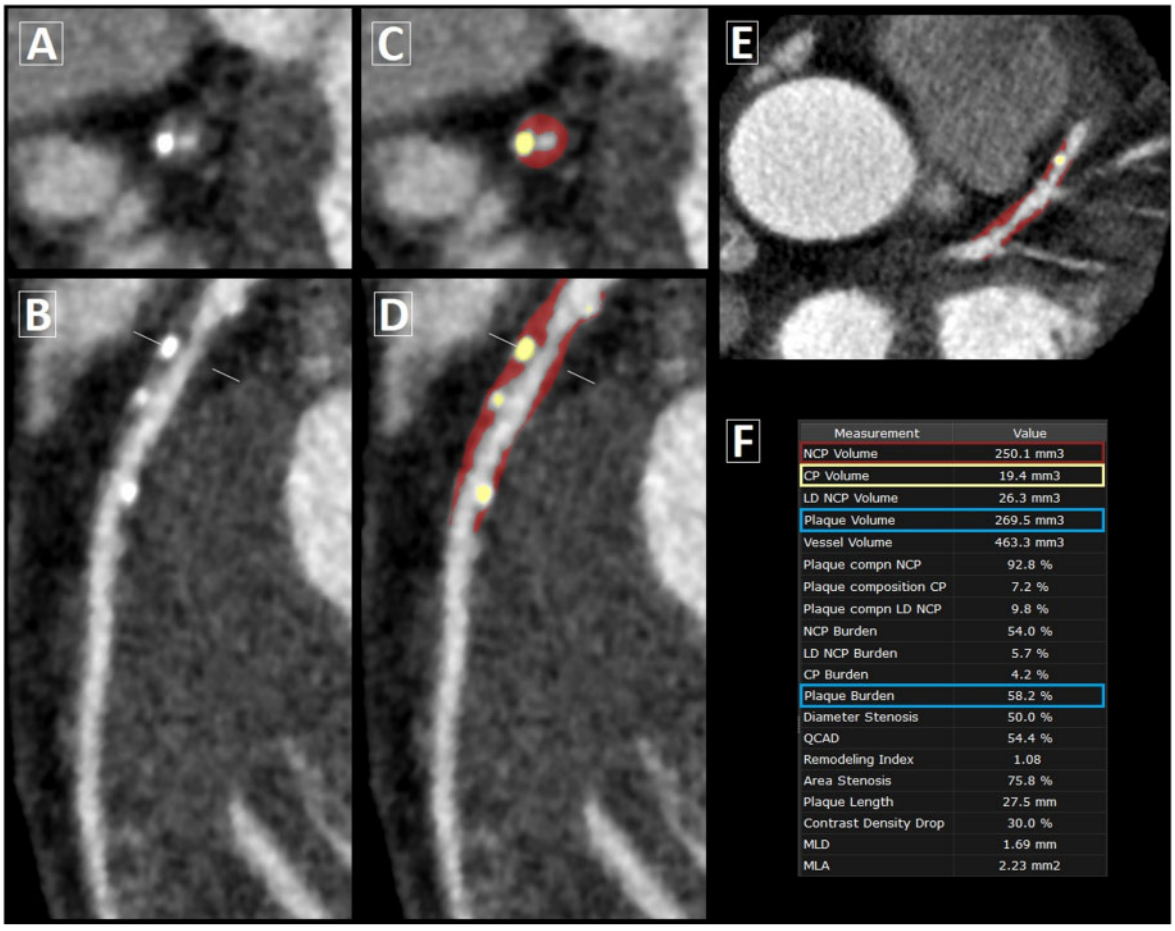

Figure 2 Semi-automated coronary plaque analysis on CCTA. Case example of plaque quantification in a 67-year-old male patient with stable CAD. (*A*) Cross-section and (*B*) curved multi-planar view of mixed plaque in the proximal-to-mid left anterior descending artery. (*C* and *D*) Corresponding views and (*E*) axial slice following semi-automated plaque analysis, with non-calcified plaque (NCP) in red overlay and calcified plaque (CP) in yellow overlay. (*F*) Plaque volume = NCP volume + CP volume; plaque burden = plaque volume × 100%/analysed vessel volume.

Table 1 Clinical, laboratory, and CCTA characteristics of the study population

	Acute MI ($n = 60$)	Stable CAD ($n = 60$)	No CAD ($n = 60$)	*P*-value
Clinical characteristics				
Age (years)	59.9 ± 11.6	60.2 ± 11.3	58.7 ± 12.8	0.82
BMI (kg/m^2)	28.3 ± 5.9	28.7 ± 5.0	28.8 ± 5.4	0.93
Male gender	52 (86.7)	52 (86.7)	52 (86.7)	1.00
Hypertension	44 (73.3)	41 (68.3)	42 (70.0)	0.71
Diabetes	15 (25.0)	13 (21.7)	12 (20.0)	0.65
Dyslipidaemia	32 (53.3)	35 (58.3)	31 (51.7)	0.46
Smoking	24 (40.0)	20 (33.3)	19 (31.7)	0.31
Family history of CAD	25 (41.7)	27 (45.0)	18 (30.0)	0.34
Baseline medications				
Antiplatelet	11 (18.3)	10 (16.7)	8 (13.3)	0.27
Statin	15 (25.0)	17 (28.3)	13 (21.7)	0.35
Beta-blocker	10 (16.7)	12 (20.0)	10 (16.7)	0.54
ACE-I or ARB	14 (23.3)	14 (23.3)	12 (20.0)	0.46
Lipids (mmol/L)				
Total cholesterol	4.9 ± 1.3	5.1 ± 1.1	5.3 ± 1.2	0.08
LDL cholesterol	3.0 ± 1.1	3.0 ± 0.9	3.5 ± 1.1	0.06
Inflammatory markers				
hs-CRP (mg/L)	9.7 (6.2–13.3)	1.8 (0–3.6)	1.4 (0–2.8)	**<0.001**
White cell count ($\times 10^9$/L)	9.1 ± 3.0	6.5 ± 1.4	5.9 ± 2.2	**<0.001**
CCTA acquisition parameters				
Heart rate (bpm)	53.9 ± 5.3	54.8 ± 8.4	56.4 ± 8.0	0.15
Tube voltage				1.00
100 kV	22 (36.7)	22 (36.7)	22 (36.7)	
120 kV	38 (63.3)	38 (63.3)	38 (63.3)	
Contrast dose (mL)	77.6 ± 11.0	76.2 ± 13.9	75.8.6 ± 9.8	0.65
Radiation dose (DLP)	284.8 ± 156.9	246.1 ± 171.4	275.2 ± 165.3	0.42
Right coronary- or codominance	56 (93.3)	54 (90.0)	55 (91.7)	0.77
CCTA segment scores				
Segment involvement score	5.8 ± 3.1	5.1 ± 2.5		0.38
Segment stenosis score	14.2 ± 7.9	9.7 ± 5.2		**0.005**
Quantitative plaque measures				
Proximal RCA plaque volume (mm^2)	140.7 ± 106.7	99.3 ± 68.0		0.13
Proximal RCA plaque burden (%)	20.9 ± 14.2	12.9 ± 7.2		**0.03**
Total coronary plaque volume (mm^2)	554.0 ± 265.4	399.9 ± 187.5		0.09
Total coronary plaque burden (%)	32.0 ± 15.5	18.4 ± 9.4		**<0.001**
EAT measurements				
EAT volume (mm^3)	97.0 ± 25.6	85.4 ± 22.1	78.2 ± 28.8	**<0.001**
EAT attenuation (HU)	-87.2 ± 4.3	-89.8 ± 4.7	-90.2 ± 4.2	0.25
PCAT attenuation (HU)	-82.3 ± 5.5	-90.6 ± 5.7	-95.8 ± 6.2	**<0.001**

Values are expressed as *n* (%), mean ± standard deviations, or median (interquartile range, 25th–75th).
BMI, body mass index; CAD, coronary artery disease; CCTA, coronary computed tomography angiography; HU, Hounsfield units; EAT, epicardial adipose tissue; hs-CRP, high-sensitivity C-reactive protein; LDL, low-density lipoprotein; MI, myocardial infarction; RCA, right coronary artery. Bold face p-values indicate statistical significance.

tissue was defined as all voxels with attenuation between -190 HU and -30 HU, and PCAT attenuation was defined as the mean CT attenuation (HU) of adipose tissue within the defined volume of interest.[6,7] As the average luminal diameter of the proximal RCA in the study population was 3.4 mm, we considered the PCAT attenuation within a volume between the vessel wall and an outer radial distance of 3 mm from the vessel wall.[6] Using the cohort-averaged proximal RCA diameter accounted for any significant individual variations due to coronary dominance[16] or the vasodilatory effects of sublingual nitroglycerine.[17] We included patients with all types of coronary dominance, given the lack of evidence regarding its influence on PCAT attenuation. In rare cases where the RCA length was <50 mm, the proximal limit for PCAT measurement was adjusted to within 0–10 mm of the RCA ostium. Coronary branches originating from the RCA and myocardial tissue adjacent to the vessel wall were excluded from automated PCAT analysis. For each proximal RCA segment,

PCAT attenuation was exported along with quantitative measures of plaque volume and plaque burden. The average processing time for automated PCAT measurement was <30 s.

Epicardial adipose tissue quantification

Epicardial adipose tissue (EAT) was defined as all adipose tissue enclosed by the visceral pericardium. EAT volume (cm^3) and attenuation (HU) were quantified from non-contrast CT images by an expert reader (J.Y.) using semi-automated software (QFAT v2.0, Cedars-Sinai Medical Center), as previously described.[18]

Laboratory analyses

Fasting blood samples were obtained from all MI patients within 48 h of admission. Laboratory results for the outpatient cohorts were obtained from a pathology database within 1 month prior to their CCTA. Total cholesterol, LDL-C, high-sensitivity C-reactive protein (hs-CRP), and total white blood cell count (WCC) were analysed by a single laboratory (Monash Pathology, Victoria, Australia) using standard techniques.

Statistical analysis

Data were tested for normality using the Shapiro–Wilk test. Continuous variables are presented as mean ± standard deviation or median (interquartile range), as appropriate. Comparisons among the three stages of CAD (MI vs. stable CAD vs. no CAD) were performed using a one-way ANOVA with *post hoc* Sidak correction for pairwise comparisons in cases of normally distributed continuous variables. For non-normally distributed continuous variables, the Kruskal–Wallis test was applied with *post hoc* Bonferroni correction for pairwise comparisons. A χ^2 or Fisher's exact test was used for categorical variables. Pearson or Spearman's rank correlations were used to assess correlations between continuous variables. Multi-variable linear regression was used to evaluate the relationship between stage of CAD and PCAT attenuation, with adjustment for age, gender, cardiovascular risk factors (diabetes, hypertension, dyslipidaemia, and smoking), EAT volume, and quantitative coronary plaque burden. We tested for interaction between clinical presentation (MI or stable CAD) and coronary plaque burden on PCAT attenuation in the regression model. We assessed the contribution of PCAT attenuation to each stage of CAD using three separate multi-variable logistic regression models, adjusting for cardiovascular risk factors and EAT volume. Statistical analysis was performed using Stata version 14.0 (StataCorp, College Station, TX, USA). A two-sided *P*-value of <0.05 was considered statistically significant.

Results

Table 1 summarizes the characteristics of the study population according to stage of CAD. There were no significant differences in age, gender, BMI, risk factors, or medications between groups.

Clinical presentation

Among patients with acute MI, 55 (92%) presented with NSTEMI and 5 (8%) with thrombolysed STEMI. The mean time from hospital admission to CCTA was 29.2 ± 8.6 h. The culprit vessel was the RCA in 10 cases (17%) and the culprit lesion was within the analysed proximal RCA segment in 5 cases (8%). The serum inflammatory markers hs-CRP and total WCC were increased in patients with MI over those with stable or no CAD (*Table 1*).

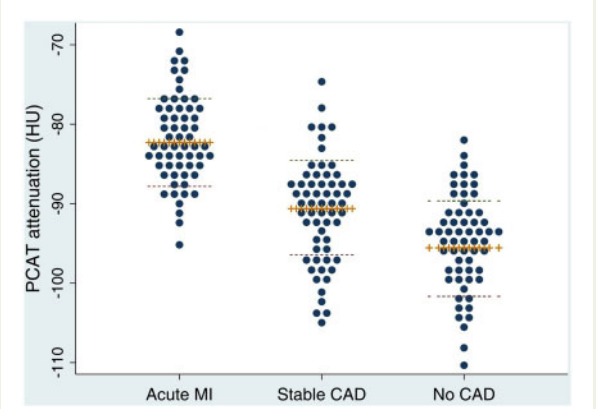

Figure 3 Dot plots of PCAT attenuation values in different stages of CAD. Plus sign markers and dashed lines represent the mean and standard deviation, respectively. PCAT attenuation was higher in patients with MI (-82.3 ± 5.5 HU) compared with patients with stable CAD (-90.6 ± 5.7 HU, $P < 0.001$) and controls with no CAD (-95.8 ± 6.2 HU, $P < 0.001$). PCAT attenuation was significantly increased in stable CAD patients over controls ($P = 0.01$).

Coronary plaque analysis

Patients with MI had a greater plaque burden in the proximal RCA and throughout the entire coronary tree compared with patients with stable CAD; plaque volume was not significantly different between the two groups (*Table 1*). Plaque burden in the proximal RCA correlated with total plaque burden throughout the coronary tree in both the stable CAD ($r = 0.869$, $P < 0.001$) and MI ($r = 0.685$, $P = 0.007$) cohorts. The extent of CAD as measured by the SIS was similar between these groups, while the SSS was higher in MI patients.

Association of PCAT attenuation with stage of CAD

PCAT attenuation was significantly higher in patients with acute MI (-82.3 ± 5.5 HU) compared with patients with stable CAD (-90.6 ± 5.7 HU, $P < 0.001$) and controls with no CAD (-95.8 ± 6.2 HU, $P < 0.001$) (*Figure 3*). There was also a significant difference in PCAT attenuation between stable CAD patients and controls ($P = 0.01$). *Figure 4* shows case examples of PCAT attenuation maps on CCTA from each of the three cohorts.

Of patients with MI, PCAT attenuation was similar whether the culprit lesion localized to the proximal RCA (n=5) or other coronary segments (n=55; -81.1 ± 5.9 vs. -82.9 ± 6.3 HU, $P = 0.518$). In patients with coronary atherosclerosis (MI and stable CAD cohorts), PCAT attenuation was increased in the presence ($n = 53$) vs. absence ($n = 67$) of plaque in the proximal RCA (-84.4 ± 6.1 vs. -88.3 ± 6.5 HU, $P = 0.015$). PCAT attenuation correlated more strongly with plaque burden within the proximal RCA ($r = 0.429$, $P < 0.001$) than with total plaque burden in the coronary tree ($r = 0.305$, $P < 0.001$).

In multi-variable linear regression analysis adjusted for age, gender, cardiovascular risk factors, EAT volume, and plaque burden in the

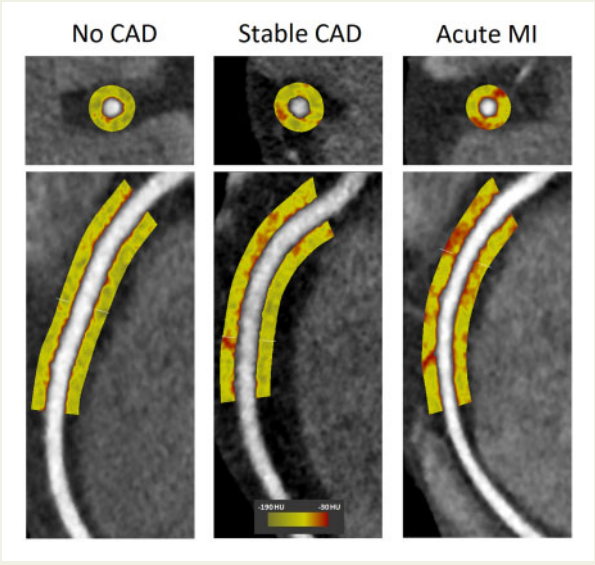

Figure 4 PCAT attenuation maps on CCTA in different stages of CAD. PCAT around the proximal 10–50 mm of the RCA is shown in cross section (upper panels) and curved multi-planar views (lower panels) in case examples of patients with no CAD, stable CAD, and acute MI. The corresponding PCAT attenuation was -105.4, -88.2, and -71.6 HU, respectively. The RCA was free of plaque in all three patients.

proximal RCA, each stage of CAD was independently associated with PCAT attenuation (*Table 2*, Model 1). The same result was observed when total coronary plaque burden was used in the model (*Table 2*, Model 2). We did not observe an interaction between clinical presentation (MI vs. stable CAD) and proximal RCA plaque burden on PCAT attenuation ($P_{interaction}$ = 0.107); the interaction term was thus removed from the regression analysis. Similarly, no interaction was noted between clinical presentation and total coronary plaque burden ($P_{interaction}$ = 0.213).

In multi-variable logistic regression adjusted for age, gender, and risk factors, an increasing PCAT attenuation was associated with MI [odds ratio (OR) 1.49, 95% CI 1.32–1.67, $P < 0.001$] (*Table 3*, Model 1). Conversely, a decreasing PCAT attenuation was independently associated with stable or no CAD (OR 0.88, 95% CI 0.80–0.96, $P = 0.004$; and OR 0.81, 95% CI 0.73–0.92, $P < 0.001$) (*Table 3*, Models 2 and 3).

EAT measures

EAT volume was higher in patients with MI compared with patients with stable CAD and controls (both $P < 0.001$); EAT attenuation did not differ significantly between the groups (*Table 1*). PCAT attenuation correlated with EAT attenuation in controls ($r = 0.622$, $P = 0.001$) and patients with stable CAD ($r = 0.295$, $P = 0.01$), however not in MI patients ($P = 0.541$). PCAT volume was not significantly different between the three groups ($P = 0.705$).

Table 2 Multi-variable linear regression—relationship between stage of CAD and PCAT attenuation

Variables	Beta coefficient[a]	95% CI		*P*-Value
Model 1—adjusted for proximal RCA plaque burden				
Constant[b]	-95.844	-105.562	-84.127	**<0.001**
Acute MI	11.907	15.508	8.307	**<0.001**
Stable CAD	4.872	2.539	7.204	**<0.001**
Age	0.007	-0.108	0.123	0.902
Female gender	-2.333	-5.263	0.597	0.118
Diabetes	-0.745	-4.256	2.765	0.675
Hypertension	-0.916	-3.873	2.040	0.541
Dyslipidaemia	0.719	-2.304	3.741	0.639
Smoking	-1.018	-3.924	1.888	0.490
EAT volume	-0.025	-0.057	0.007	0.124
Proximal RCA plaque burden	0.086	-0.013	0.186	0.089
Model 2—adjusted for total coronary plaque burden				
Constant[b]	-96.449	-101.872	-91.026	**<0.001**
Acute MI	12.676	7.985	17.368	**<0.001**
Stable CAD	5.923	2.794	9.052	**0.039**
Age	0.023	-0.094	0.139	0.703
Female gender	-2.750	-5.703	0.204	0.068
Diabetes	-0.404	-3.936	3.127	0.821
Hypertension	-0.815	-3.836	2.206	0.595
Dyslipidaemia	1.180	-1.833	4.193	0.440
Smoking	-1.204	-4.139	1.731	0.419
EAT volume	-0.020	-0.052	0.013	0.226
Total coronary plaque burden	0.019	-0.081	0.119	0.789

CAD, coronary artery disease; EAT, epicardial adipose tissue; MI, myocardial infarction; PCAT, pericoronary adipose tissue; RCA, right coronary artery. Bold face p-values indicate statistical significance.
[a]Dependent variable: PCAT attenuation (HU).
[b]Denotes a 60-year-old male control patient with no CAD or risk factors.

Discussion

In this cross-sectional study, we show that PCAT attenuation, a novel imaging biomarker of coronary inflammation, increases across three distinct stages of CAD (no disease vs. stable CAD vs. acute MI). This association is independent of age, gender, risk factors, EAT volume, and coronary plaque burden.

Inflammation plays a critical role in atherogenesis and atherothrombosis. Deposition of LDL and its oxidation in the coronary arterial wall triggers an inflammatory response, with recruitment of monocytes and T cells into the intima.[1] Pro-inflammatory cytokines released by these immune cells then contribute to the progression of atherosclerotic plaque.[1] In patients with stable CAD, circulating levels of hs-CRP and interleukin-6 associate with risk of MI and cardiac death.[19] Further, as shown by the present analysis and prior investigators,[20] serum hs-CRP levels are higher in acute MI vs. stable CAD. On PET-CT imaging, ^{18}F-fluorodeoxyglucose uptake is greater in ACS culprit lesions compared with lesions in stable patients.[3] However, circulating inflammatory markers are not specific for coronary inflammation,[21,22] and PET-CT is limited by cost and clinical

Table 3 Multi-variable logistic regression—association of PCAT attenuation with each stage of CAD

Variables	Odds ratio	95% CI	*P*-Value
Model 1—acute MI			
PCAT attenuation (HU)	1.49	1.32–1.67	**<0.001**
Age (years)	1.03	0.95–1.08	0.26
Male gender	1.00	0.74–1.29	0.68
Diabetes	1.37	0.39–2.17	0.49
Hypertension	1.13	0.99–2.04	0.08
Dyslipidaemia	1.09	1.03–2.98	**0.03**
Smoking	1.16	1.10–2.23	**0.03**
EAT volume (cm^3)	1.03	1.01–1.06	**0.02**
Model 2—stable CAD			
PCAT attenuation (HU)	0.88	0.80–0.96	**0.004**
Age (years)	1.02	0.98–1.07	0.18
Male gender	0.97	0.47–1.38	0.65
Diabetes	0.78	0.19–2.18	0.73
Hypertension	1.31	0.38–2.60	0.67
Dyslipidaemia	1.09	1.02–2.13	**0.04**
Smoking	0.94	0.60–0.98	**0.01**
EAT volume (cm^3)	0.98	0.95–1.00	0.08
Model 3—no CAD			
PCAT attenuation (HU)	0.81	0.73–0.92	**<0.001**
Age (years)	0.91	0.86–1.09	0.34
Male gender	0.98	0.57–1.43	0.59
Diabetes	0.67	0.12–2.84	0.65
Hypertension	0.69	0.33–1.20	0.39
Dyslipidaemia	0.74	0.43–1.48	0.19
Smoking	0.94	0.29–3.22	0.96
EAT volume (cm^3)	0.95	0.92–1.03	0.47

CAD, coronary artery disease; EAT, epicardial adipose tissue; HU, Hounsfield units; PCAT, pericoronary adipose tissue. Bold face p-values indicate statistical significance.

availability.[23] Hence, a routine, non-invasive method of quantifying the local coronary inflammatory status is highly desirable.

It is established that coronary inflammation propagates into PCAT, with pro-inflammatory cytokines from the arterial wall inhibiting local adipogenesis.[6] This can be detected as an increased CT attenuation of PCAT on CCTA, and measurement of PCAT attenuation around the proximal RCA is the most standardized and reproducible per-patient level approach.[6–8,15] The proximal RCA has the highest volume of surrounding adipose tissue[24] and an absence of confounding non-fatty structures such as side branches, coronary veins, or myocardium.[6] PCAT attenuation around the proximal RCA has been used as a biomarker of global coronary inflammation,[6,8] with a high value predicting cardiac mortality.[8] Goeller *et al.*[7] showed longitudinal changes in PCAT attenuation around the proximal RCA to associate with changes in non-calcified plaque burden in the entire coronary tree. The same authors previously reported a higher PCAT attenuation around culprit lesions compared with non-culprit lesions in patients with ACS and the highest grade stenosis lesions of patients with stable CAD.[25] Our study is the first to quantify PCAT attenuation around the proximal RCA in patients with MI and compare these measurements with matched patients with stable or no CAD.

The present analysis showed PCAT attenuation around the proximal RCA to distinguish patients with acute MI from those with stable CAD, independently of total coronary plaque burden. Based on these findings, we hypothesize that the increased PCAT attenuation in MI may reflect a greater local inflammatory burden associated with plaque disruption. PCAT attenuation was not influenced by the distribution of culprit lesions (RCA vs. non-RCA), indicating that PCAT surrounding the proximal RCA may undergo phenotypic changes in response to plaque rupture anywhere in the coronary tree. Prior evidence suggests that patients with MI have pan-coronary arterial inflammation and instability.[26–28] Mauriello *et al.*[26] demonstrated inflammatory infiltrates in stable plaques throughout the entire coronary vascular bed in an *ex vivo* study of patients dying from MI. Kubo *et al.*[27] reported multiple optical coherence tomography-derived vulnerable plaques in non-culprit vessels in the setting of MI. Here, we demonstrate that PCAT attenuation around the proximal RCA as a non-invasive imaging biomarker may potentially quantify this acute, widespread coronary inflammation.

In our study, patients with stable CAD had a higher PCAT attenuation than controls with no CAD, perhaps reflecting the chronic, low-grade coronary inflammation associated with atherosclerosis.[1] Consistent with the report by Goeller *et al.*,[7] we found PCAT attenuation around the proximal RCA to correlate more strongly with plaque burden in this coronary segment than with total plaque burden in the coronary tree, highlighting the direct 'cross-talk' between the coronary arterial wall and immediately adjacent pericoronary adipocytes.[6,29] Despite this, we showed a significant difference in PCAT attenuation between patients with stable CAD and controls after adjustment for plaque burden in the proximal RCA. Moreover, we observed no significant interaction effect between clinical presentation with stable CAD and proximal RCA plaque burden on PCAT attenuation. Antonopoulos *et al.*[6] also demonstrated the ability of PCAT attenuation around the proximal RCA to detect significant CAD in any vessel, independently of the presence of obstructive RCA disease. Our results lend further support to the hypothesis that PCAT attenuation surrounding the proximal RCA represents inflammatory changes in the entire coronary vasculature.

While there was a correlation between PCAT attenuation and EAT attenuation in controls and stable CAD patients, we found no significant differences in EAT attenuation between the three stages of CAD. This suggests that the coronary arteries may exert a stronger pathophysiological influence on PCAT due to its anatomical proximity compared with distant epicardial adipocytes. Indeed, studies have reported conflicting results on the association of EAT attenuation with coronary plaque,[30] myocardial ischaemia,[31] and MI,[32] highlighting the important phenotypic differences between PCAT and non-PCAT components of EAT. Furthermore, histological evidence demonstrates that adipocytes immediately adjacent to the coronary arterial wall are smaller with less intracellular lipid compared with adipocytes at a radial distance of 20 mm from the coronaries, likely due to the local influence of inflammatory mediators in the pericoronary microenvironment.[6]

In summary, PCAT attenuation around the proximal RCA as a biomarker of global coronary inflammation can distinguish patients in different stages of CAD. This highly reproducible quantitative measure is obtained on routine CCTA at no extra cost or radiation exposure. The ability to reliably detect coronary inflammation on a per-patient

level has important treatment implications, especially in those with stable CAD who have a substantial residual inflammatory risk despite statin therapy.[33] Recent evidence has shown both novel[5] and established[34]anti-inflammatory agents to significantly reduce the rate of recurrent cardiovascular events in such patients. PCAT attenuation could potentially identify individuals with a high coronary inflammatory burden who may benefit from these targeted therapies in addition to aggressive secondary prevention. This metric could also be used to monitor the inflammatory status of patients post-MI, whereby achieving a normal value may become a therapeutic target. Systemic biological therapy for the treatment of psoriasis has recently been shown to modulate PCAT attenuation,[15] and future studies should examine the effects of conventional and novel therapies for CAD on this imaging biomarker.

Limitations

Ours was a single-centre and single-vendor study of a relatively small patient cohort who underwent CCTA, hence the results require confirmation in a larger population scanned with different CT acquisition parameters. This was a cross-sectional analysis, and longitudinal studies are needed to examine the natural history of PCAT attenuation following acute MI. The PCAT measurement used represents the mean CT attenuation of adipose tissue within the defined volume of interest and is not weighted for technical or biological factors. Further, we applied the cohort-averaged proximal RCA diameter of 3 mm as a standardized approach for PCAT analysis instead of patient-specific vessel diameters. We did not directly measure coronary inflammation, however recent studies have shown PCAT attenuation to associate with biopsy-proven vascular inflammation in patients undergoing cardiac surgery.[6] Finally, the spatial resolution of CT may limit PCAT assessment in small amounts of adipose tissue and adjacent to heavy coronary calcification which may exert partial volume averaging effects.

Conclusion

PCAT attenuation as a quantitative measure of coronary inflammation reliably distinguishes different stages of CAD. This lends support to its potential role in guiding the implementation of preventative or targeted therapies. Future studies should assess whether this imaging biomarker can track patient responses to treatment for CAD.

Data availability

The data underlying this article cannot be shared publicly to protect the privacy of individuals that participated in the study. The data will be shared on reasonable request to the corresponding author.

Acknowledgements

A.L., S.J.N, and D.T.W. are supported by grants from the National Health and Medical Research Council (Australia). N.N. is supported by a grant from the National Heart Foundation of Australia. D.D. is supported by grants from the National Heart, Lung, and Blood Institute [1R01HL133616 and 1R01HL148787-01A1].

Conflict of interest: none declared.

References

1. Libby P. Inflammation in atherosclerosis. *Arterioscler Thromb Vasc Biol* 2012;**32**:2045–51.
2. Stefanadis C, Toutouzas K, Tsiamis E, Stratos C, Vavuranakis M, Kallikazaros I *et al.* Increased local temperature in human coronary atherosclerotic plaques: an independent predictor of clinical outcome in patients undergoing a percutaneous coronary intervention. *J Am Coll Cardiol* 2001;**37**:1277–83.
3. Rogers IS, Nasir K, Figueroa AL, Cury RC, Hoffmann U, Vermylen DA *et al.* Feasibility of FDG imaging of the coronary arteries: comparison between acute coronary syndrome and stable angina. *JACC Cardiovasc Imaging* 2010;**3**:388–97.
4. Joshi NV, Vesey AT, Williams MC, Shah AS, Calvert PA, Craighead FH *et al.* 18F-fluoride positron emission tomography for identification of ruptured and high-risk coronary atherosclerotic plaques: a prospective clinical trial. *Lancet* 2014;**383**:705–13.
5. Ridker PM, Everett BM, Thuren T, MacFadyen JG, Chang WH, Ballantyne C *et al.* Antiinflammatory therapy with canakinumab for atherosclerotic disease. *N Engl J Med* 2017;**377**:1119–31.
6. Antonopoulos AS, Sanna F, Sabharwal N, Thomas S, Oikonomou EK, Herdman L *et al.* Detecting human coronary inflammation by imaging perivascular fat. *Sci Trans Med* 2017;**9**:1–12.
7. Goeller M, Tamarappoo BK, Kwan AC, Cadet S, Commandeur F, Razipour A *et al.* Relationship between changes in pericoronary adipose tissue attenuation and coronary plaque burden quantified from coronary computed tomography angiography. *Eur Heart J Cardiovasc Imaging* 2019;**20**:636–43.
8. Oikonomou EK, Marwan M, Desai MY, Mancio J, Alashi A, Hutt Centeno E *et al.* Non-invasive detection of coronary inflammation using computed tomography and prediction of residual cardiovascular risk (the CRISP CT study): a post-hoc analysis of prospective outcome data. *Lancet* 2018;**392**:929–39.
9. Thygesen K, Alpert JS, Jaffe AS, Chaitman BR, Bax JJ, Morrow DA *et al.*; ESC Scientific Document Group. Fourth universal definition of myocardial infarction (2018). *Eur Heart J* 2019;**40**:237–69.
10. Jacobson TA, Ito MK, Maki KC, Orringer CE, Bays HE, Jones PH *et al.* National lipid association recommendations for patient-centered management of dyslipidemia: part 1–full report. *J Clin Lipidol* 2015;**9**:129–69.
11. Wong DT, Soh SY, Ko BS, Cameron JD, Crossett M, Nasis A *et al.* Superior CT coronary angiography image quality at lower radiation exposure with second generation 320-detector row CT in patients with elevated heart rate: a comparison with first generation 320-detector row CT. *Cardiovasc Diagn Ther* 2014;**4**:299–306.
12. Leipsic J, Abbara S, Achenbach S, Cury R, Earls JP, Mancini GJ *et al.* SCCT guidelines for the interpretation and reporting of coronary CT angiography: a report of the Society of Cardiovascular Computed Tomography Guidelines Committee. *J Cardiovasc Comput Tomogr* 2014;**8**:342–58.
13. Min JK, Shaw LJ, Devereux RB, Okin PM, Weinsaft JW, Russo DJ *et al.* Prognostic value of multidetector coronary computed tomographic angiography for prediction of all-cause mortality. *J Am Coll Cardiol* 2007;**50**:1161–70.
14. Dey D, Schepis T, Marwan M, Slomka PJ, Berman DS, Achenbach S. Automated three-dimensional quantification of noncalcified coronary plaque from coronary CT angiography: comparison with intravascular US. *Radiology* 2010;**257**:516–22.
15. Elnabawi YA, Oikonomou EK, Dey AK, Mancio J, Rodante JA, Aksentijevich M *et al.* Association of biologic therapy with coronary inflammation in patients with psoriasis as assessed by perivascular fat attenuation index. *JAMA Cardiol* 2019;**4**:885–91.
16. Dodge JT Jr, Brown BG, Bolson EL, Dodge HT. Lumen diameter of normal human coronary arteries. Influence of age, sex, anatomic variation, and left ventricular hypertrophy or dilation. *Circulation* 1992;**86**:232–46.
17. Takx RAP, Suchá D, Park J, Leiner T, Hoffmann U. Sublingual nitroglycerin administration in coronary computed tomography angiography: a systematic review. *Eur Radiol* 2015;**25**:3536–42.
18. Dey D, Suzuki Y, Suzuki S, Ohba M, Slomka PJ, Polk D *et al.* Automated quantitation of pericardiac fat from noncontrast CT. *Invest Radiol* 2008;**43**:145–53.
19. Held C, White HD, Stewart RAH, Budaj A, Cannon CP, Hochman JS *et al.* Inflammatory biomarkers interleukin-6 and C-reactive protein and outcomes in stable coronary heart disease: experiences from the STABILITY (Stabilization of Atherosclerotic Plaque by Initiation of Darapladib Therapy). *Trial. J Am Heart Assoc* 2017;**6**:1–14.
20. Zebrack JS, Anderson JL, Maycock CA, Horne BD, Bair TL, Muhlestein JB. Usefulness of high-sensitivity C-reactive protein in predicting long-term risk of death or acute myocardial infarction in patients with unstable or stable angina pectoris or acute myocardial infarction. *Am J Cardiol* 2002;**89**:145–9.

21. Tataru MC, Heinrich J, Junker R, Schulte H, von Eckardstein A, Assmann G *et al.* C-reactive protein and the severity of atherosclerosis in myocardial infarction patients with stable angina pectoris. *Eur Heart J* 2000;**21**:1000–8.
22. Brevetti G, Giugliano G, Brevetti L, Hiatt William R. Inflammation in peripheral artery disease. *Circulation* 2010;**122**:1862–75.
23. Robson PM, Dey D, Newby DE, Berman D, Li D, Fayad ZA *et al.* MR/PET imaging of the cardiovascular system. *JACC Cardiovasc Imaging* 2017;**10**: 1165–79.
24. Maurovich-Horvat P, Kallianos K, Engel LC, Szymonifka J, Fox CS, Hoffmann U *et al.* Influence of pericoronary adipose tissue on local coronary atherosclerosis as assessed by a novel MDCT volumetric method. *Atherosclerosis* 2011;**219**: 151–7.
25. Goeller M, Achenbach S, Cadet S, Kwan AC, Commandeur F, Slomka PJ *et al.* Pericoronary adipose tissue computed tomography attenuation and high-risk plaque characteristics in acute coronary syndrome compared with stable coronary artery disease. *JAMA Cardiol* 2018;**3**:858–63.
26. Mauriello A, Sangiorgi G, Fratoni S, Palmieri G, Bonanno E, Anemona L *et al.* Diffuse and active inflammation occurs in both vulnerable and stable plaques of the entire coronary tree: a histopathologic study of patients dying of acute myocardial infarction. *J Am Coll Cardiol* 2005;**45**:1585–93.
27. Kubo T, Imanishi T, Kashiwagi M, Ikejima H, Tsujioka H, Kuroi A *et al.* Multiple coronary lesion instability in patients with acute myocardial infarction as determined by optical coherence tomography. *Am J Cardiol* 2010;**105**:318–22.
28. Asakura M, Ueda Y, Yamaguchi O, Adachi T, Hirayama A, Hori M *et al.* Extensive development of vulnerable plaques as a pan-coronary process in patients with myocardial infarction: an angioscopic study. *J Am Coll Cardiol* 2001;**37**:1284–8.
29. Margaritis M, Antonopoulos AS, Digby J, Lee R, Reilly S, Coutinho P *et al.* Interactions between vascular wall and perivascular adipose tissue reveal novel roles for adiponectin in the regulation of endothelial nitric oxide synthase function in human vessels. *Circulation* 2013;**127**:2209–21.
30. Lu MT, Park J, Ghemigian K, Mayrhofer T, Puchner SB, Liu T *et al.* Epicardial and paracardial adipose tissue volume and attenuation - association with high-risk coronary plaque on computed tomographic angiography in the ROMICAT II trial. *Atherosclerosis* 2016;**251**:47–54.
31. Hell MM, Achenbach S, Schuhbaeck A, Klinghammer L, May MS, Marwan M. CT-based analysis of pericoronary adipose tissue density: relation to cardiovascular risk factors and epicardial adipose tissue volume. *J Cardiovasc Comput Tomogr* 2016;**10**:52–60.
32. Mahabadi AA, Balcer B, Dykun I, Forsting M, Schlosser T, Heusch G *et al.* Cardiac computed tomography-derived epicardial fat volume and attenuation independently distinguish patients with and without myocardial infarction. *PLoS One* 2017;**12**:e0183514.
33. Ridker PM. Residual inflammatory risk: addressing the obverse side of the atherosclerosis prevention coin. *Eur Heart J* 2016;**37**:1720–2.
34. Tardif J-C, Kouz S, Waters DD, Bertrand OF, Diaz R, Maggioni AP *et al.* Efficacy and safety of low-dose colchicine after myocardial infarction. *N Engl J Med* 2019; **381**:2497–505.